

<연구논문>

## 한정된 공간에서의 희석 고분자 용액의 흐름

손영곤<sup>†</sup> · 박오옥\*

한국과학기술원 화학공학과  
(1992년 3월 31일 접수)

### Flow of Dilute Polymer Solutions in the Confined Geometry

Young Gon Son<sup>†</sup> and O Ok Park\*

*Department of Chemical Engineering Korea Advanced Institute of Science and Technology  
Technology, 373-1 Kusung, Yusung, Taejeon 305-701, Korea  
(Received March 31, 1992)*

#### 요 약

한정된 공간 속을 희석 고분자 용액이 흐를 때 그 공간의 특성 길이가 고분자의 그것과 비슷한 경우에는 실험적으로 무한 공간에 비하여 점도가 작게 됨을 보였다. 잔탄 겔 용액과 폴리아크릴 아미드 용액이 원통형 다공을 가진 고분자 막을 통해 흐를 때의 점도를 뉴턴 영역 뿐 아니라 비뉴턴 영역에서도 한꺼번에 측정할 수 있는 흐름 장치를 만들어 실험하였다. 뉴턴 점도는 다공의 크기가 줄어들수록 줄어드는 경향을 보였는데 이는 두 특성 길이의 비로서 설명할 수 있었다. 비뉴턴 점도 영역에서의 지표(power law index)는 폴리아크릴 아미드 용액에서는 차이가 발견되지 않았으나 잔탄 겔 용액에서는 다공의 크기가 감소할수록 점점 작은 값을 보였다. 이것은 두 고분자 사슬의 경직성 차이에 기인된다 하겠다. 결론적으로 벽 근처에 분자 크기 정도의 고분자 회박 영역이 존재하고 그 영역내에서는 고분자 사슬의 배향 구조가 제한적이라고 하는 이론적 설명과 부합되는 결과를 얻었다.

**Abstract**—Polymer solutions flowing through small pores of which length scale is comparable with polymers were experimentally demonstrated to have reduced apparent viscosities from those obtained in unbounded media. Simple, but efficient rheometric configuration was designed to obtain both Newtonian and shear thinning viscosities simultaneously over a wide range of shear rate for Xanthan and Polyacrylamide solutions flowing through a well-defined cylindrical pore. Zero shear viscosities were found to decrease with decreasing size of pores for both solutions, which can be correlated with relative size of polymers compared with that of confining geometry. But power law index in the shear thinning region were not much changed for polyacrylamide solution and decreased for xanthan solution. It could be due to the flexibility difference between two polymers. There seems to be a depletion layer of one molecular length near the wall, where the conformation of the polymer chains is restricted as theories suggested.

**Keywords:** Dilute polymer solutions, flexibility, confining geometry, depletion layer, Xanthan, Polyacrylamide

<sup>†</sup>Current address: Cheil Wool Co. Polymer Research center

\*To whom any correspondence should be addressed

## 1. Introduction

Flow of polymer solutions in the porous media has been an interesting subject not only because of the practical purpose such as enhanced oil recovery but also because of academic reason. It is obvious that flows in confined geometry is different from those in the infinite domain. Such problem has been studied by several workers both experimentally [1-6] and theoretically [7-11]. Almost every work on the experiments concerned either a complicated geometry of small size or cylindrical one of large size compared with length scale of the polymer chain under consideration. Here it may be helpful to classify two distinct cases based on the relative size of polymer to that of confining geometry. If they are comparable with each other, it is easy to formulate theoretical problem with help of molecular models such as elastic dumbbell for flexible chains and rigid dumbbell model for rigid chains. However, its experimental verification is somewhat complicated due to the difficulty of obtaining well defined flows in such a small scale. In this context, Chauveteau [12] performed excellent experiments on flows of Xanthan solutions through a well-defined cylindrical micro pores to obtain that shear viscosity decreases as size of pore decreases because of the concentration depletion layer formed near the wall of pore. On the other hand, if the relative size of confining geometry is much larger than that of polymers, then situation is totally different. Viscosity reduction was observed on a rather too large scale to be explained with depletion layer of molecular scale. Cohen and Metzner [13] did carry out such flowing experiments of several polymer solutions through small capillary to see apparent viscosities decrease as the diameter of the capillary decreases. They interpreted it as an apparent slip and developed a systematic analysis to calculated not only thickness of slip layer but also slip velocity. Here we are going to restrict ourselves to the former case to demonstrate that relative molecular scale to size of confining geometry will play the major role to determine the viscosity reduction and experimental results can

be compared with known theoretical predictions. Furthermore it will be shown that flexible polymer shows slightly different behaviors compared with those of rigid one flowing in the confined geometry. Simple, but efficient rheometric design will be used to measure the both Newtonian and shear thinning viscosities simultaneously, and a proper method for data analysis will be performed to see those differences.

## 2. Experiments

### 2.1. Materials

Polymers used for this work are Xanthan and Polyacrylamide, which are representing rigid and flexible polymer chains respectively. Xanthan was purchased from Sigma Co. as practical grade and its weight average molecular weight  $M_w$  is about  $6.2 \times 10^6$ . Polyacrylamide was obtained from Aldrich Co. as powder, of which  $M_w$  is  $5.5 \times 10^6$ . Water is used as solvents for both polymers with appropriate quantity of NaCl. In case of Xanthan, 5 g/l of NaCl was chosen for salinity, 20 g/l was for polyacrylamide in order to maintain the expected chain conformations for both polymers. Solvation was done with a magnetic stirrer with minimum speed in order to reduce any possibility of degradation of polymer chains. After that they were filtered through membrane with a low flow rate to get rid of any solid particles, suspensions or microgel. Concentration was chosen 400 ppm for Xanthan and 500 ppm for polyacrylamide. For the confined geometry, Polycarbonate nucleopore membrane was used, which is known to have a well-defined cylindrical pore. Nominal diameters of the pores were 0.6-10  $\mu\text{m}$  and thickness 3-10  $\mu\text{m}$  shown in Table 1. Actual diameters measured by SEM were slightly smaller than nominal ones and a few pores were found to be only slightly connected so that they can be considered to be separated. Thickness of the membranes were measured to be same as nominal thickness by the supplier. In order to avoid any possibility of adsorption of the polymer on the wall of the pores during flowing in such a fine pore, chemical treatment was done before experiment as suggested by Co-

**Table 1.** Dimension of the pore membranes used (unit in  $\mu\text{m}$ )

Nominal Diameter	Diameter Measured	Thickness
10	9.7	10
8	7.8	7
5	5.6	10
3	2.7	9
2	1.9	10
1	0.96	10
0.8	0.72	9
0.6	0.62	10

hen and Meztner [13]. 2% dichlorodimethylsilane was added to the solvent of 95% ethanol plus 5% distilled water. This solution was flowed for a day before experiment.

## 2.2. Experimental Apparatus and procedure

In order to obtain the shear viscosities over a wide range, a simple, but efficient rheometer was specially designed (Fig. 1). Conventional capillary rheometer will give us only one point on the plot of shear rate-shear viscosity, but with this rheometer a series of data can be obtained by a single experimental run. Viscosity in the infinite domain for reference were obtained by using a capillary having either 0.5 mm in diameter and 6.07 m in length or 1 mm in diameter and 0.1, 0.2, 0.3 m in length. Temperature of the solution was maintained at 25°C with on-off temperature controller in the water bath. Rheometer is consisted of two vertical cylinders connected by flowing cell, which can be either a capillary for water, or membrane with pore for polymer solutions. Since the pressure drop between two tubes is very small so that the height and its time variation was checked with a cathetometer, of which the accuracy is up to  $10^{-3}$  mm. In case of membrane cell, stainless grid was used to support it.

Basic argument of obtaining flow rates and pressure drops is very simple. Time variation of the height difference will give us the flow rate and height difference itself will be linear in pressure drop. Then a proper mathematical scheme will give us the functional relationship between shear rate and shear viscosity, which will be explained

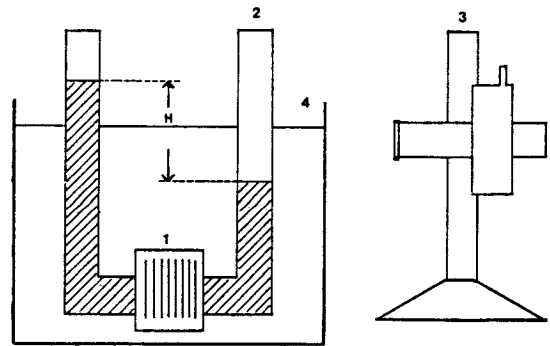


**Fig. 1.** Experimental Apparatus 1) Flow device (pore membrane, capillary) 2) Measuring Cylinder 3) Cathetometer 4) Temperature Bath.

later. For accurate experiment vertical tube setting is necessary, which was done by levelmeter.

## 2.3. Data Analysis

Main reason for the design of a new rheometer is to reduce the number of experiments. A proper scheme for data analysis is necessary in order to have shear rate-shear viscosity relationship from height-time relationship measured experimentally. First of all it was assumed to give us a quasi-steady state, fully developed flow of Hagen-Poiseuille type through the capillary. When Newtonian fluid is flowed through a capillary, it is very simple to obtain the viscosity. Flow rate ( $Q$ ) is proportional to the pressure drop ( $\Delta p$ ) so that

$$Q = \pi r_c^4 \Delta p / 8 \mu L_c \quad (1)$$

where  $r_c$  and  $L_c$  are radius and length of the capillary and  $\mu$  is the Newtonian viscosity.  $Q$  and  $\Delta p$  are related to  $H$  and  $dH/dt$  as followings:

$$Q = -1/2 \pi R^2 dH/dt \quad (2)$$

$$\Delta p = \rho g H \quad (3)$$

where  $\rho$  is density and  $g$  is gravitational acceleration constant. Thus, it can be converted to the relationship between  $H$  and  $dH/dt$ .

$$dH/dt = -(r_c^4 \rho g / 4 \mu L_c R^2) H \quad (4)$$

From the initial condition to say  $H = H_0$  at  $t = 0$ , following equation is obtained easily.

$$\ln[H/H_0] = -(r_c^4 \rho g / 4 \mu L_c R^2) t \quad (5)$$

Thus a plot of  $\ln(H)$  vs  $t$  can supply us the viscosity at high shear rate as shown in Fig. 2. In case of porous membrane, geometric factors are different from those in eq. (5). The result is:

$$\ln[H/H_0] = -(\epsilon_p A_m r_p^4 \rho g / 4 \mu L_m R^2) t \quad (6)$$

Here  $\epsilon_p$  is pore density in the membrane and  $A_m$  and  $L_m$  are area and length of the membrane respectively.  $r_p$  is the radius of the pore. Eq. (4) can be used to determine the pore density with known viscosity in Newtonian region.

If the viscosity of the polymer solution is dependent upon shear rate imposed, then analysis is a little longer, but simple relationship can be obtained for each case. It is based on the Rabinowitch's equation to relate flow rate and pressure drop data to wall shear rate ( $\gamma_w$ ) and wall shear stress ( $\tau_w$ ):

$$\gamma_w = [3Q + \Delta p \, dQ/d\Delta p] / \pi r_c^3 \quad (7)$$

$$\tau_w = r_c \Delta p / 2L_c \quad (8)$$

If eqs. (2) and (3) are substituted into eqs. (7) and (8), non-Newtonian viscosity can be obtained.

$$\gamma_w = (R^2 / 2r_c^3) H \{3H'/H + H''/H'\} \quad (9)$$

$$\tau_w = (r_c \rho g / 2L_c) H \quad (10)$$

$$\mu = (\rho g r_c^4 / LR^2) \{3H'/H + H''/H'\}^{-1} \quad (11)$$

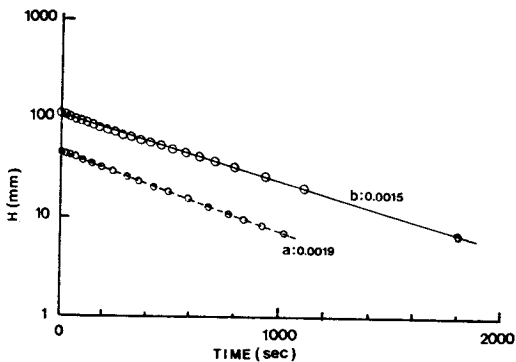


Fig. 2.  $\ln(H)$  vs.  $t$  for Newtonian Fluid in viscometer in Fig. 1. a) High shear rate b) Low shear rate

where  $H' = dH/dt$  and  $H'' = d^2H/dt^2$ . Thus  $H(t)$  data will supply us not only shear rate but also shear stress. If polymer solutions are flowed through the fine pore, the coefficients are changed accordingly.

$$\gamma_w = (R^2 / 2A_m \epsilon_p r_p^3) H \{3H'/H + H''/H'\} \quad (12)$$

$$\tau_w = (r_p \rho g / 2L_m) H \quad (13)$$

$$\mu = (A_m \epsilon_p \rho g r_p^4 / L_m R^2) \{3H'/H + H''/H'\}^{-1} \quad (14)$$

If these equations are applied to the Newtonian region, evaporation of the solvent causes a large change in height compared with that of flow since shear rate is too low. But it can be proven not to affect on the above analysis if evaporation occurs at same rate from both sides.

### 3. Results and Discussions

Fig. 3 shows shear viscosities of Xanthan solution of 400 ppm. It shows a typical thinning behavior from shear rate 5/sec in capillary flow, which is thought to be the case of infinite domain compared with molecular scale. Power law index at shear thinning is 0.734. Polyacrylamide solution of 500 ppm shows similar but much weaker thinning behavior with power law index 0.948. Viscosities of Xanthan solutions in fine pore are shown in Fig. 3 along with capillary data. As radius of pore reduces apparent Newtonian viscosity decreases as expected. But 1  $\mu$ m pore shows different

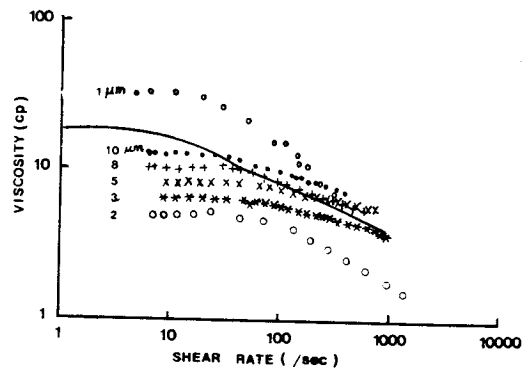


Fig. 3. Shear Viscosity of Xanthan 400 ppm Solution, Solid line: infinite domain, Others: fine pore membranes.

tendency due to the difficulty of flowing into such a small region with Xanthan of characteristic length  $L_r = 1.5 \mu\text{m}$ . Similar phenomena was observed by Chauveteau [12]. Evaluation of characteristic length of Xanthan will be discussed later. Polyacrylamide solution always has decreasing tendency as radius of pore decreases as shown in Fig. 4. In case of Xanthan solutions, slope of shear thinning region decreases as radius of pore decreases up to  $5 \mu\text{m}$ , which means apparent power law index will increase accordingly. If the radius of pore is reduced further this tendency is reversed. These are listed in Table 2. It could be due to the end effect of the large pore case since the length of the pore is not enough to reach a fully

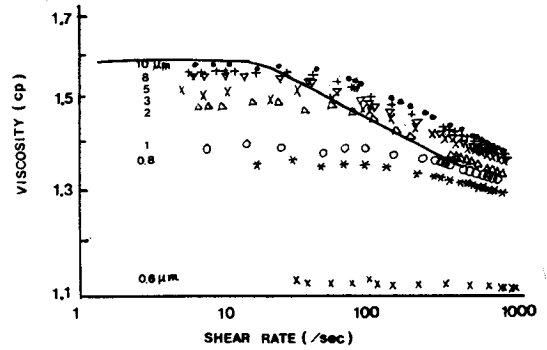


Fig. 4. Shear Viscosity of Polyacrylamide 500 ppm Solution, Solid line: infinite domain, Others: fine pore membranes.

Table 2. Xanthan solution of 400 ppm

Pore Size $\mu\text{m}$	Zero-shear Viscosity cp	Power Law Index	Relative Size* $e = L_r/2r_p$	Dimensionless Viscosity	Diffusivity $D_r \times 100$
capillary	7.13	.734	0.00	1.00	11.2
9.7(10)	4.92	.779	0.16	0.64	2.68
7.8( 8)	3.99	.756	0.19	0.49	1.93
5.6( 5)	3.24	.866	0.27	0.37	1.08
2.6( 3)	2.52	.778	0.58	0.25	0.85
1.9( 2)	2.30	.576	0.78	0.21	1.00
.96( 1)	—	.334	1.56	—	—

\* $L_r = 1.5 \mu\text{m}$  from eq. (16).

( ) means nominal size.

Table 3. Polyacrylamide solution of 500 rpm

Pore Size $\mu\text{m}$	Zero-shear Viscosity cp	Power Law Index	Relative Size* $e = L_r/2r_p$	Dimensionless Viscosity
capillary	1.59	.948	0.00	1.00
9.7(10)	1.57	.952	0.04	0.97
7.9( 8)	1.55	.954	0.05	0.94
5.6( 5)	1.54	.957	0.07	0.92
2.6( 3)	1.51	.963	0.15	0.86
1.9( 2)	1.47	.960	0.21	0.81
.96( 1)	1.38	.967	0.41	0.65
.72(.8)	1.34	.979	0.54	0.50
.52(.6)	1.12	.995	0.75	0.34

\* $L_r = 0.195 \mu\text{m}$  from eq. (18).

( ) means nominal size.

developed flow. Therefore power law index seems to decrease as pore diameter decreases if fully developed flow can be achieved. Polyacrylamide solutions show a different characteristics to have a slightly increasing power law index as radius of pore decreases, but it may be safe to conclude to have same power law index within experimental errors. These are tabulated in Table 3. Now zero-shear viscosity will be compared with known theoretical predictions. In order to do that, the molecular dimensions of the polymers should be first evaluated.

For rigid polymer like Xanthan, it was suggested to evaluate macromolecular dimension from intrinsic viscosity data (Benoit *et al.* [14]). If aspect ratio  $p$  is large enough ( $p > 50$ ), then viscosity factor  $v_0 = [\eta]_0 / v_{sp}$  can be approximated by power law:

$$v_0 = 0.159 p^{1.801} \quad (15)$$

Here  $v_{sp}$  is the specific volume, equal to 0.62 for oligosaccharides. Aspect ratio  $p$  was calculated as 508 according to the experimental intrinsic viscosity of Xanthan, 7360 cm<sup>3</sup>/g. Once aspect ratio is given, equivalent length of Xanthan,  $L_r$  is estimated from

$$L_r^3 = (45/2\pi N_A) [\eta] M_w (\ln 2p - 0.5) \quad (16)$$

where  $N_A$  is Avogadro's number.  $L_r$  was calculated as 1.5  $\mu\text{m}$ , which is nearly consistent with 1.15  $\mu\text{m}$  reported elsewhere (Chun *et al.* [15]). Zero shear viscosity due to polymer chains can be compared with theoretical research (Park and Fuller [10]) as shown in Fig. 5. Our experimental data and Chauveteau [12] data are all in a single curve when dimensionless polymer length based on pore size. But theoretical predictions of viscosity reduction are much underestimated. The possible reason is that simple shear flow was assumed instead of Poiseuille flow for the theoretical prediction based on rigid dumbbell model, where the inhomogeneous flow effect was excluded.

For flexible polymer chain like polyacrylamide, Flory-Fox equation tells us the relationship between intrinsic viscosity and radius of gyration:

$$[\eta] = 6^{2/3} \phi \langle s^2 \rangle^{3/2} / M_w \quad (17)$$

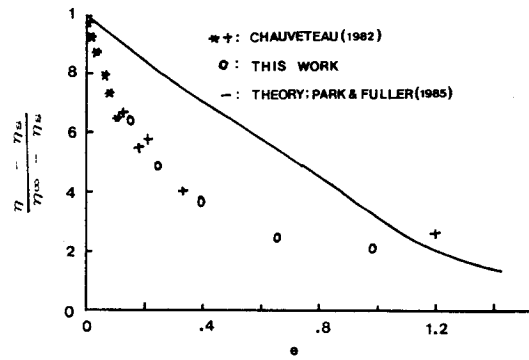


Fig. 5. Zero-shear viscosity of Polymer Contribution vs. dimensionless length of Xanthan, Solid line: Theoretical Calculation based on Park & Fuller (1985), \*: Chauveteau (1982) data in glass bead packing, +: Chauveteau (1982)'s data in porous membranes, O: This work.

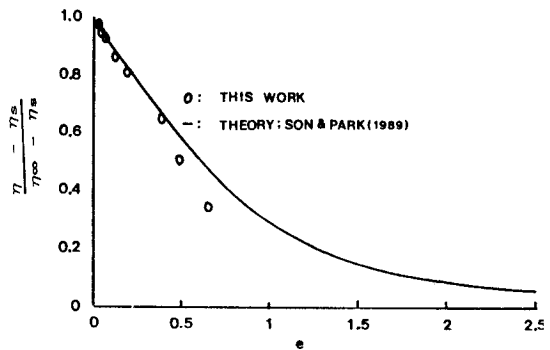


Fig. 6. Zero-shear viscosity of Polymer Contribution vs. dimensionless length of Polyacrylamide, Solid line: Theoretical Calculation based on Son & Park (1989), O: This work.

Here  $\phi$  is Flory Fox parameter,  $2.5 \times 10^{23} \text{ mol}^{-1}$  and  $\langle s^2 \rangle^{1/2}$  is root mean square radius of gyration. With experimental value of intrinsic viscosity  $[\eta] = 1143 \text{ cm}^3/\text{g}$  and known  $M_w = 5.5 \times 10^6$ , radius of gyration  $\langle s^2 \rangle^{1/2}$  was obtained 0.12  $\mu\text{m}$ . Thus characteristic length of polyacrylamide  $L_r$  would be

$$L_r = (8/3)^{1/2} \langle s^2 \rangle^{1/2} = 0.195 \mu\text{m} \quad (18)$$

Based on this length scale, dimensionless viscosity increment due to polymer chains is plotted against relative polymer length to that of confining geometry in Fig. 6. Experimental data was compared with known theoretical calculation (Son and Park

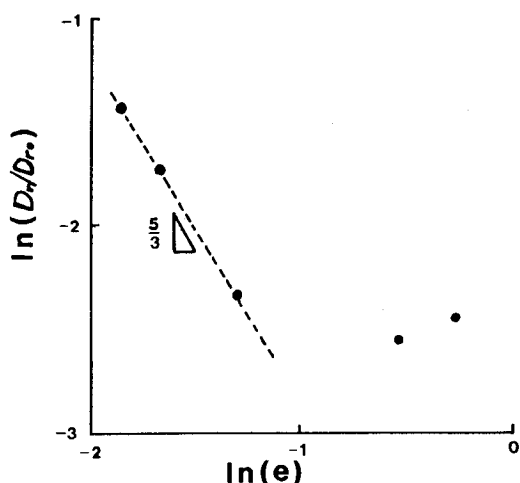


Fig. 7. Rotational Diffusivity vs. dimensionless length of Xanthan.

[11]), where elastic dumbbell model polymer in rectilinear flow was considered. Agreement between theory and experiment is fairly good.

One other thing we can think of is that rigid polymer chains in confining geometry have lower rotational diffusivity than in infinite domain. From the transition point from Newtonian to shear thinning it may be possible to estimate such reduction of rotational diffusivity, which are tabulated in last column of Table 3.  $\log(D_r/D_{r0})$  vs  $e=L_r/r_p$  is plotted in Fig. 7.

### Conclusions

Flows of polymer solutions in confined geometry is governed by relative length scale of polymer chains to characteristic length of pores, when they are comparable. In such a case, flexibility of polymer chains plays a role for not only Newtonian viscosity but also power law index in shear thinning region.

### Nomenclature

$A_m$  : area of the membrane  
 $D_r$  : rotational diffusivity  
 $D_{r0}$  : rotational diffusivity in the infinite domain

$e$  : relative size ( $L_r/2r_p$ )  
 $g$  : gravitational acceleration constant  
 $H$  : height  
 $H_0$  : height at  $t=0$   
 $H'$  :  $dH/dt$   
 $H''$  :  $d^2H/dt^2$   
 $L_c$  : length of the capillary  
 $L_m$  : length of the membrane  
 $L_r$  : characteristic length of the polymers  
 $M_w$  : molecular weight  
 $N_A$  : Avogadro's number  
 $p$  : aspect ratio  
 $Q$  : flow rate  
 $r_c$  : radius of the capillary  
 $r_p$  : radius of the pore  
 $R$  : radius of the tube  
 $\langle s^2 \rangle^{1/2}$  : root mean square radius of gyration  
 $t$  : time  
 $v_0$  : viscosity factor  
 $v_{sp}$  : specific volume  
 $\epsilon_p$  : pore density  
 $\mu$  : viscosity  
 $\rho$  : density  
 $\gamma_w$  : wall shear rate  
 $\tau_w$  : wall shear stress  
 $[\eta]$  : intrinsic viscosity  
 $[\eta]_0$  : intrinsic viscosity at zero shear rate  
 $\phi$  : Flory-Fox parameter

### References

1. F.W. Smith, *J. Pet. Technol.*, **22**, 148 (1970).
2. W.B. Smith, *J. Pet. Technol.*, **25**, 1307 (1973).
3. L. Desremaux, G. Chauveteau and M. Martin, Coll. A.R.T.E.P., Paper No. 28, June 7-9, 1971.
4. M.T. Szabo, Paper No. 4028 presented at the SPE meeting, San Antonio, October 8-11, 1972.
5. J.M. Maerker, *J. Pet. Technol.*, **2**, 1307 (1973).
6. G. Chauveteau and J.C. Moulu, *Eur. Symp. E.O.R.*, Edinburgh, July 5-7, 1978, pp. 65-82.
7. P.O. Brunn, *Rheol. Acta* **15**, 23-29 (1976).
8. J.H. Aubert and M. Tirrell, *J. Chem. Phys.*, **77**, 553-561 (1982).
9. W. Stasiak and C. Cohen, *J. Chem. Phys.*, **78**, 553-559 (1983).
10. O. O. Park and G.G. Fuller, *J. Non-Newtonian Fluid Mech.*, **15**, 309-329 (1985).

11. Y.G. Son and O O. Park, *Hwahak Konghak*, **27**(6), 759-766 (1989).
12. G. Chauveteau, *J. Rheol.*, **26**, 111-142 (1982).
13. Y. Cohen and A.B. Metzner, *J. Rheol.*, **29**, 67-104 (1985).
14. M. Bernoit, L. Freund and G. Sparch in "Poly- $\alpha$ -amino acids," G.D. Fasman, Ed., Marcel Dekker, New York (1967).
15. M.-S. Chun, O O. Park and J.K. Kim, *Korean J. Chem. Eng.*, **7**(2), 126-137 (1990).